Article

Assessment of the Human Retinal Neural Selectivity to Square Gratings' Orientation with the Multifocal and Pattern Electroretinograms

Ana Amorim-de-Sousa [1],*, Paulo Fernandes [1], Noberto López-Gil [2], António Queirós [1] and José M. González-Méijome [1]

1   Clinical and Experimental Optometry Research Laboratory (CEORLab), Physics Center of Minho and Porto Universities (CF-UM-UP), University of Minho, Gualtar, 4710-057 Braga, Portugal
2   Faculty of Optics and Optometry, University of Murcia, Espinardo, 30100 Murcia, Spain
*   Correspondence: ana.amorim.sousa@gmail.com

Abstract: The retinal response to particular orientations might start a signaling cascade of events that help to modulate eye growth and respond to myopia control treatments. The purpose of this study was to investigate the retinal electrical activity in response to grids of different spatial orientations. The multifocal (mfERG) and pattern (PERG) ERG responses of nine eyes (spherical equivalent of -0.45 ± 1.15 D; mean age of 32.9 ± 7.7 years) were recorded with four grids (1.2 cpd) oriented at $60°$, $90°$, $120°$ and $180°$ under pupils' dilation. The mfERG was analyzed by retinal eccentricity, quadrants and meridians with the same orientation of the grids. The response density of mfERG, the amplitudes of PERG and the implicit times of each peak from both tests were analyzed. The grid's orientation did not evoke different implicit times in both tests. All retinal meridians showed higher response density with grids of parallel orientation to the meridian and lower response density with perpendicularly oriented grids. These differences were statistically significant in the horizontal and $60°$ meridians ($p < 0.050$). PERG response did not change with the grids' orientations. The mfERG was sensitive to detect changes in the outer retinal activity with variations in stimulus orientation. The paradigm of meridional analysis of mfERG results might be more sensitive to orientation changes than the traditional analysis by rings, quadrants or hemifields.

1. Introduction

The visual system features against-the-rule astigmatism across the horizontal meridian of the retina and with-the-rule astigmatism across the vertical meridian [1–3]. Previously, Atchison et al. reported a higher impact of peripheral astigmatism on the horizontal rather than vertical meridian [4]. Together with the spatial frequency, oblique astigmatism may also have a potential role in the emmetropization process. Oblique incidence or off-axis astigmatism will lower the image quality in the periphery, and this degradation might be more significant for different orientations and resolution objects. According to previous studies, Sturm's interval—the range between tangential and sagittal focal points—of oblique astigmatism and their orientations might generate potential cues used by the eye to detect blur and control its growth [5,6]. One of the hypotheses relies on the possibility of the peripheral retina to estimate and use the magnitude and sign of off-axis astigmatism to control the emmetropization process [7].

Nevertheless, the mechanism by which the retina may detect the relative position of the sagittal and tangential focal surfaces working as a regulator effect on ocular growth is still not known. Different eye growth patterns were observed in primate eyes according to the relative position of the tangential and sagittal focal lengths [8]. This relies on the assumption that the retina tends to reposition itself toward the most posterior focal position

(sagittal focal) in the presence of mixed astigmatisms [9]. Some studies have reported an association between the development of myopia in school-aged children with astigmatism, especially against-the-rule astigmatism, hypothesizing astigmatism as a disrupting factor of emmetropization for eye growth [1,10].

Myopia management strategies have been effective in myopia control in humans [11–13]. In addition to the myopic shift of the peripheral refraction, most myopia control devices increase substantially the incidence of oblique astigmatism, showing a negative increase in the relative J0 astigmatism (against-the-rule astigmatism) in the horizontal meridian of the retina [14–16], while in the vertical retinal meridian, the relative cartesian astigmatism (J0) increases positively (with-the-rule astigmatism) [3].

Whether or not the stimulation of the retina using different spatial frequencies that maximize contrast in a particular orientation might elicit a variable level of retinal activity, as well as its role in guiding the eye towards emmetropia, remain unknown. This retinal activity can be measured with electrophysiological techniques [17–22]. In the human eye, different electroretinogram (ERG) methodologies were applied to assess the retinal response to stimuli of varying spatial frequency [2,21,23–26]. However, the changes observed were not yet analyzed to evaluate the possible relationship between the distinct cellular layers of the retina. The authors hypothesize that the retinal activity might change differently with the stimulus orientation in different meridional directions. These changes might start a signaling cascade of events that span from the retina, through the choroid and into the scleral tissue to modulate the eye growth and the response to myopia control treatments. It is further hypothesized that changes in the activity of cells from the outer retina [27,28] would be reproduced in the response of inner cellular groups responsible for the integration of contrast at the retinal level [29,30].

The purpose of the present pilot study was to investigate the global and local retinal activity in the outer and inner retina in response to different spatial orientations of grid patterns. Beyond the common analysis of the retinal activity by eccentricity and quadrants, this study also aims to examine the retinal sensitivity of different meridians to the stimulus orientation.

2. Materials and Methods

2.1. Study Design and Subjects

This cross-sectional study consisted of evaluating both multifocal (mfERG) and pattern (PERG) ERG responses when presenting grids of four orientations. The protocol was approved by the Ethics Subcommittee for Health and Life Sciences of the University of Minho and followed the guidelines of the Declaration of Helsinki. After detailed information about the study and before enrollment, all participants provided written informed consent.

The volunteers were recruited from an academic population and selected according to the following inclusion criteria: age between 18 and 45 years old, a spherical equivalent between +1.00 diopters (D) and −2.00 D, astigmatism up to 1.00 D, high-contrast (99%) visual acuity of at least 0.00 logMAR (logarithm of the minimum angle of resolution), ocular media transparency and no ocular or systemic diseases or any previous ocular surgical procedure. Before the ERG assessment, subjects underwent an optometric evaluation to ensure compliance with the inclusion criteria. All measurements were performed in a single session.

For sample characterization purposes, the high- (99%) and low- (10%) contrast visual acuity (HCVA and LCVA, respectively) and the refractive error were registered. The refractive error is represented in vectorial components (M as spherical equivalent, J0 as cartesian astigmatism and J45 as oblique astigmatism) calculated according to the following equations:

$$\text{M} = Sphere + \frac{Cylinder}{2} \tag{1}$$

$$J0 = \frac{Cylinder}{2} \times \cos(2axis) \tag{2}$$

$$J45 = \frac{Cylinder}{2} \times \sin(2axis) , \tag{3}$$

2.2. ERG Assessment

The electrophysiological measurements (mfERG and PERG) were recorded with the RETIport/scan21™ (Roland Consult, Brandenburg, Germany). Pupils were fully dilated with 2 drops of 1% Phenylephrine (Davinefrina, DÁVI II—Farmacêutica S.A, Lisbon, Portugal) 25–30 min before the recordings. Subjects were optically corrected for the display distance for both mfERG (~28 cm) and PERG (at 1 m), as recommended by the International Society for Clinical Electrophysiology of Vision standards protocols [31,32]. An active Dawson–Trick–Litzlkow (DTL)-plus electrode was placed on the lower conjunctiva in contact with the cornea. The stimuli were displayed in a 19-inch RGB LCD monitor (ProLite B1980SD, iiyama, Nagano, Japan). The built-in camera of the system allows for monitoring the participant's fixation during the experiment. All the required mfERG measurements were obtained before the PERG measurements, and the different conditions were randomly recorded with both techniques.

The mfERG response is a result of the activity of photoreceptors and bipolar cells. This technique allows for evaluating the cells' response to the presence and absence of light [32]. A stimulus pattern of 61 black and white hexagons scaled with eccentricity was displayed at approximately 28 cm (~+3.00 D vergence) from the eye, covering up to 56° of the retina. Subjects should fixate on a central red cross in the middle of the pattern stimuli. Each hexagon followed an m-sequence flickering between white and dark at a frame rate of 60 Hz. The first negative (N1) and positive (P1) of the first-order kernel of the mfERG waveforms were analyzed by concentric areas—central retina (fovea; from 0 to 4.80°), mid-peripheral retina (parafovea; 4.80° to 21.62°) and peripheral retina (periphery; 21.62° to 54.10°) (Figure 1a), both by quadrants—top-right, top-left, bottom-left and bottom-right quadrants (Figure 1b), and by meridians—horizontal, vertical, 60° and 120° (Figure 1c). The implicit time of N1 and P1 peaks (measured from the onset of the stimulus to the peak of interest) in milliseconds (ms) and the response density (ratio of the amplitude measured between peaks and troughs by analysis area) of P1 in nano volts per square degree (nV/deg^2) of the curves were analyzed (Figure 1d) [32].

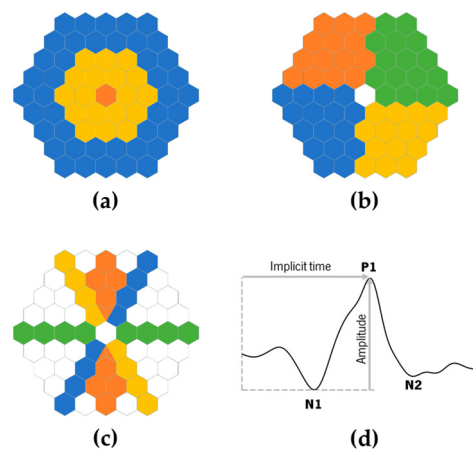**Figure 1.** The multifocal electroretinogram (mfERG) response was analyzed by (**a**) eccentricity in three concentric rings (macula in orange, mid-periphery in yellow and periphery in blue), (**b**) quadrants (top-right in green; top-left in orange; bottom-left in blue; bottom-right in yellow) and (**c**) four meridians (horizontal—green; 60°—blue; vertical—orange; 120°—yellow). (**d**) Typical mfERG wave curve [33].

The PERG response essentially concerns the ganglion cells, driven by the response of the photoreceptors and bipolar cells from the earlier stages of the retinal visual integration to generate the action potentials that abandon the eye to the brain. This is a global response of the area covered by the stimulus to changes in contrast and reflects the integrity of the optics and the cellular path from photoreceptors to ganglion cells [31]. The pattern stimulation was a black and white (98% contrast) reversing checkerboard (Figure 2a), with a check size of 0.8°, presented at a reversal rate of 4.29 reversals per second (2.15 Hz) at 1 m of the subject (+1.00 D vergence). Vergence distance was compensated with a frameless trial lens and considering the spherical equivalent refractive error of the subject. Central fixation with a red cross was used. Each measurement accounts for two consecutive waveforms with a sweep time (period of analysis) of 180 ms that are off-line averaged and then analyzed. The implicit times of peaks N35, P50 and N95 in milliseconds (ms) and the amplitudes of P50 (trough of N35 to the peak of P50) and N95 (peak P50 to the trough of N95) in microvolts (μV) were used for analysis (Figure 2b).
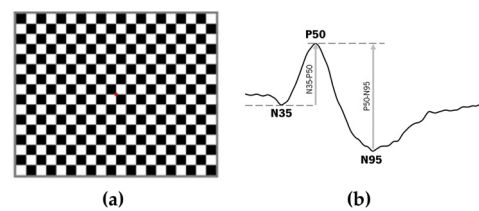

(a) (b)

Figure 2. (**a**) PERG stimulus is a reversed black and white checkerboard at 4.29 reversals per second with a check size of 0.8°. The reversal patterns allow for eliciting a curve response similar to that of (**b**) [31].

2.3. Evaluation Conditions

mfERG and PERG protocols were recorded with four square grids of 1.2 cycles per degree (cpd) oriented at 60°, 90°, 120° and 180° (from the researcher's point of view; Figure 3). The recordings with the four orientations were performed in random order. All grids were printed in transparent films and placed over the monitor's display. In a preliminary study, the effect of using a total transparent film over the monitor's display on the luminance and illuminance conditions was considered. The transparency reduced the stimulus maximum luminance by $10.85 \pm 0.58\%$ and illuminance by $1.65 \pm 1.41\%$ compared to no transparent film over the monitor. Since the comparison between grids did not include baseline recordings (no transparent film over the monitor), and all grids present the same attenuation effect, the measurements are comparable among them.
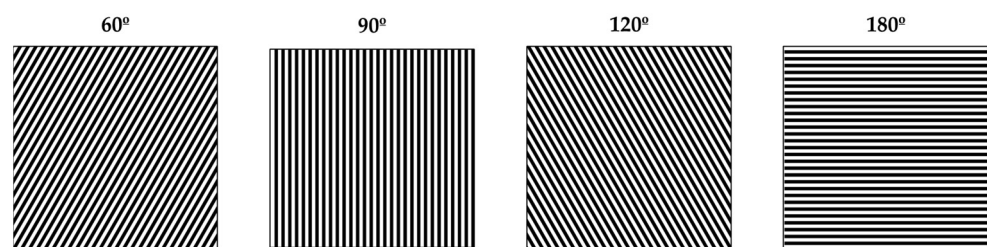
Figure 3. Four square gratings of 1.2 cpd with different orientations (60°, 90°, 120° and 180°) of the grid were placed in the monitor, overlapping the mfERG and PERG stimuli pattern.

To ensure that the contrast of the stimuli would not differ between the grids printed in the transparent films, the maximum (white) and minimum (dark) luminance of the screen (L_{max} and L_{min}, respectively, in cd/m^2) of each grid was measured (10 measurements) in the same recording conditions of mfERG and PERG. The contrast C was calculated through the Michelson contrast equation:

$$C = \frac{L_{max} - L_{min}}{L_{max} + L_{min}} \times 100 \tag{4}$$

2.4. Statistical Analysis

Sample size calculations based on a coefficient variation of at least 20% in the mfERG response density of P1 [34], superior to the repeatability of 15% of the RETIscan device found by Mazinani et al. [35], to ensure a statistical power of at least 80% with a statistical significance set at 5%. GPower software (version 3.1.9.4, Germany) calculations resulted in a minimum sample size of 3 subjects to fulfil those requirements.

Statistical analysis was conducted using the SPSS v26.0 software (IBM, Inc., New York, NY, USA). Since the sample size was small, and the parameters of the electrophysiological response do not exhibit a normal distribution, with marked inter-subject variations, statistical analysis was carried out using non-parametric statistical tests. Values are represented as the median and interquartile range (IQR). Friedman's test was used for multiple comparisons with post hoc Bonferroni correction applied for pairwise comparison when the multiple comparisons showed statistically significant differences between grid orientation. The level of statistical significance for 80% of statistical power was set at $p \leq 0.050$.

3. Results

3.1. Impact of Illumination Conditions

The C without any grid was 98.7%. The maximum and minimum luminance of both ERG stimuli were 95.76 ± 3.26 cd/m^2 and 1.11 ± 0.13 cd/m^2, respectively. Since mfERG and PERG were recorded at different distances to the monitor, the mean illuminances were also different between techniques. Before acquisitions, the luminance and illuminance of the monitor with each grid of different orientations with the mfERG and PERG stimuli were measured (Table 1).

Table 1. Luminance, illuminance and contrast C (mean $\pm$ SD) of the screen stimulus during mfERG and PERG recordings with each grid of different orientation.

	Luminance (cd/m^2)	Illuminance (lux)		C (%)
		mfERG	**PERG**	
60°	47.43 ± 0.62	103.12 ± 3.37	-	97.88 ± 0.09
90°	50.81 ± 0.78	105.10 ± 3.20	139.83 ± 0.53	97.43 ± 0.07
120°	48.47 ± 0.62	102.21 ± 3.29	-	97.83 ± 0.06
180°	47.02 ± 1.12	108.28 ± 2.48	136.10 ± 0.53	97.73 ± 0.09

cd/m^2—candela per square meter; mfERG—multifocal electroretinogram; PERG—pattern electroretinogram; C—contrast.

The luminance, illuminance and contrast between grids of different orientations were very similar. This allows for excluding possible changes in the electrophysiological responses since the amplitude of the mfERG [36,37] and PERG [29,38] decrease with the illuminance and luminance levels.

3.2. Sample Characteristics

Ten subjects (4 female and 6 male) with ages between 24 and 45 years completed the study. Only one eye was randomly evaluated. The data from one female participant were not considered for analysis due to inadequate signal in the mfERG protocols. For this, the results concern the analysis of the data from nine subjects (5 right eyes, 4 left eyes). Table 2 shows the descriptive characteristics of the sample analyzed.

Table 2. Descriptive characteristics of the sample (in mean ± SD).

Gender	3 women 6 men
Age (years)	32.9 ± 7.7
M (D)	−0.45 ± 1.15
J0 (D)	0.05 ± 0.35
J45 (D)	0.00 ± 0.03
HCVA (logMAR)	−0.08 ± 0.08
LCVA (logMAR)	0.08 ± 0.06
Mydriatic Pupil Diameter (mm)	7.55 ± 0.46

M—spherical equivalent of the refractive error; J0—cartesian astigmatism; J45—oblique astigmatism; D—diopters; HCVA—high-contrast visual acuity; LCVA—low-contrast visual acuity; logMAR (logarithm of Minimum Angle of Resolution); mm—millimeters.

3.3. mfERG Response

The multiple comparisons between the grids' orientations did not show any statistically significant differences in N1 and P1 implicit times. Table 3 shows the median and interquartile range (IQR) values of the response density (nV/deg^2) for each retinal area with each orientation.

Table 3. P1 response density (median [IQR], in nV/deg^2) of each retinal area after mfERG recordings. The right column regards the statistical significance (*p*-value) of the multiple comparisons Friedman test between orientations.

		Grids Orientation				*p*-Value
		60°	**90°**	**120°**	**180°**	
	Total retina	9.48 [1.05]	11.57 [4.82]	10.49 [3.77]	10.55 [5.70]	0.706
Eccentricity	Fovea	85.60 [27.80]	73.86 [28.10]	81.13 [54.74]	82.21 [18.29]	0.314
	Parafovea	18.70 [9.20]	21.92 [10.02]	21.36 [13.94]	25.91 [8.16]	0.081
	Periphery	7.84 [1.00]	8.48 [3.91]	8.33 [4.77]	7.97 [4.66]	0.506
Quadrants	Top-Right	12.52 [2.72]	12.57 [4.65]	12.00 [2.99]	12.87 [3.38]	0.392
	Top-Left	12.14 [5.11]	14.61 [7.88]	14.54 [7.20]	12.69 [11.20]	0.115
	Bottom-Left	10.49 [6.18]	14.42 [4.19]	10.13 [6.48]	12.69 [1.95]	0.204
	Bottom-Right	10.81 [4.80]	12.06 [5.04]	14.00 [8.14]	14.18 [5.35]	0.072
Meridians	Horizontal	15.19 [11.06]	11.27 [2.43]	18.79 [7.90]	19.64 [2.89]	0.001 *
	Vertical	13.57 [3.84]	19.61 [6.71]	13.33 [7.06]	13.19 [7.11]	0.392
	60°	15.30 [6.81]	12.46 [4.72]	12.38 [3.46]	16.51 [12.30]	0.035 *
	120°	10.02 [3.53]	14.10 [8.06]	12.02 [5.22]	15.86 [16.05]	0.042 *

* Statistically significant differences by multiple comparisons (Friedman test, $p \leq 0.050$).

In general, the 60°-oriented grid elicited lower P1 RD, while 180° grids elicited the highest P1 RD, except at fovea (Table 3). The multiple comparison tests did not show statistically significant differences between the orientations in the overall retinal response, nor for different eccentric areas and quadrants of the retina. Nevertheless, distinct behaviors were observed in the retinal meridians according to orientation, with statistically significant differences in horizontal, 60° and 120° meridians according to grids orientation (Table 3). Figure 4a,b plot the median values of the P1 RD obtained at each meridian and quadrant of the retina, respectively, according to the orientation of the grids, from 60° to 180°.
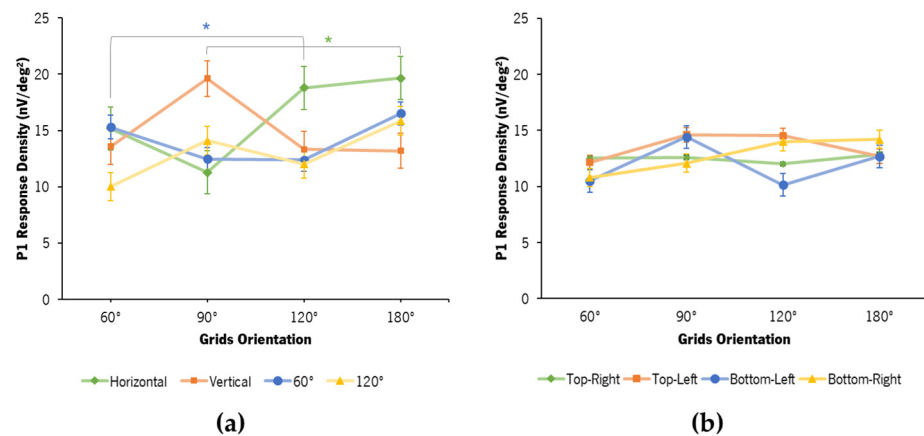
Figure 4. P1 response density (median) of the (**a**) retinal meridians and (**b**) quadrants from the mfERG according to the grid's orientation (from 60° to 180°). Post hoc Bonferroni corrections showed a statistically significant difference in the horizontal (*) and 60° (*) meridians between parallel and perpendicular grids to the meridian (90° vs. 80°; and 60° vs. 120°, respectively). Error bars represent the standard error. Refer to Table 3 for numerical values of interquartile ranges (IQR).

The multiple comparisons showed statistically significant differences between orientations in the horizontal meridian (Q(3) = 16.200, p = 0.001), the 60° meridian (Q(3) = 8.600, p = 0.035) and the 120° meridian (Q(3) = 8.200, p = 0.042). The post hoc analysis with Bonferroni corrections showed that, in the horizontal meridian of the retina, the 180° grid elicited the highest RD, while 90° elicited the lowest RD (median difference of 7.77 nV/deg^2 [12.30], p = 0.002). Similarly, in the 60° meridian, the post hoc analysis showed that the parallel grid of 60° elicited a higher RD compared to the perpendicular 120° grid (median difference of 2.92 nV/deg^2 [5.35], p = 0.021)—as seen in Figure 4a. The post hoc analysis of the 120° meridian did not show statistically significant differences. Although there were no statistically significant differences in the vertical and 120° meridians between orientations, the behavior was similar to that of the horizontal and 60° meridians. They also showed lower P1 RD with the corresponding grid of opposite orientation to the meridian itself (180° and 60°, respectively). From an equivalent perspective, considering that retinal meridians are part of retinal quadrants, this effect was already slightly perceptible in the P1 RD analysis in most quadrants, except in the bottom-left quadrant (Figure 4b).

3.4. PERG Response

The median PERG curves with the four grid orientations (60°, 90°, 120° and 180°) are represented in Figure 5. The 60°- and 120°-oriented grids showed delayed N35 and P50 peaks and a negative shift in amplitude compared with the grids oriented at 90° and 180°. The Friedman analysis showed that the differences in the implicit times and amplitudes between orientations were not statistically significant.
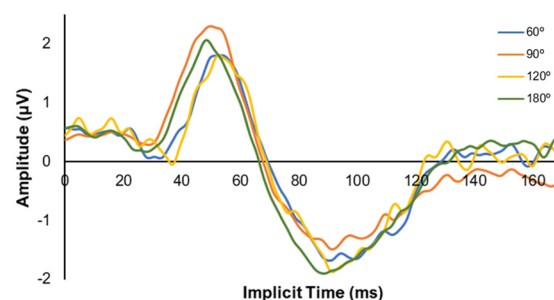

Figure 5. Median PERG curves with the four grid's orientations.

4. Discussion

The present work evaluated the changes in the electrophysiological response of the outer (mfERG) and inner retina (PERG) for different spatial square grid orientations. The mfERG response density of the horizontal retinal meridian was significantly higher with the 180° grid and minimum with the 90° grid. Although the statistical analysis did not yield significant differences, this effect was also observed in the remaining meridians of the retina. The response density of each meridian was higher with grids of parallel orientation to the meridian, while the lowest response density occurred with the grid of perpendicular orientation. The response density of the retinal quadrants to the orientation of grids resembles that of the retinal meridians, although it is less clear. On the other hand, the PERG response did not differ between the four grid orientations.

The radial distribution of ganglion cells throughout the retina is thought to be a major factor in the mechanisms of orientation preference, as their neural selectivity for task resolution gives preference to parallel grids over perpendicular grids [39–42]. This is called the meridional effect, whose stimuli oriented radially along the meridian are better resolved than stimuli oriented in other directions [40]. The findings of Venkataraman et al. [42] showed better detection and resolution acuities with parallel-oriented grids and worse with perpendicular-oriented grids in all retinal meridians analyzed, consistent with the meridional effect assumption. In the inner retina, some ganglion cells that are radially oriented also show preferential orientation with peripheral contrast maximization of grids [5,39,40]. The meridional effect mechanism supports the findings of the current results from the analysis of mfERG since each meridian was more sensitive (higher response densities) to grids of the same orientation and less sensitive (lower response densities) to grids of opposite orientation. As assumed by the meridional effect mechanism, the detection of the orientation of a grid is not restricted only in its alignment zone to a single orientation channel, but rather to multiple channels sensitive to different orientations, resulting in a summation of cellular sensitivity to different orientations [40–42]. As a result, a grid will be detected not only by the neural channel sensitive to that orientation, but also by the most efficient neural channel sensitive to its perpendicular orientation [40].

The response of the retinal quadrants partially showed this meridional effect, although this was not so evident. Each quadrant embeds cells radially distributed and oriented in an approximately 90° range, so the response of a single quadrant would result from the response summation of each of the orientation-sensitive channels in that area. Considering this, the summation of the response of cells whose orientation varies within 90° would mask the meridional effect. The analysis of the mfERG response by rings of different eccentricities comprises the sum of the response of retinal cells oriented within a range of 360°. Consequently, the meridional sensitivity caused by the radial orientation of the cells will be even less noticeable, as shown in the results of this experiment. Therefore, the analysis of the retinal response by quadrants or eccentric rings shows up to be less sensitive to radially oriented stimulus rather than the retinal response analysis by meridians.

The peripheral retina might play a crucial role in myopia progression and control [12,43–46]. The quality of the peripheral image is dominated by off-axis astigmatism and radially oriented aberrations (e.g., coma). These factors might interfere with the detection of perpendicular grids and with the orientational preference mechanisms, such as the meridional effect. The meridional detection and preference tasks depend on optical and neural sensitivities. Howland suggested that retinal circuits with cells sensitive to different orientations could be involved in detecting both sagittal and tangential positions of oblique astigmatism [7]. He also highlighted that the lack of resolution in the peripheral retina may not be directly involved in detecting defocus, but rather in distinguishing those different radial and tangential orientations of the grids [7]. In myopic eyes, the presence of astigmatism opposite to the meridional direction was observed [3,47]. Atchison et al. observed an increase in J0 negative values across the horizontal visual field with the level of myopia, especially in the nasal retina [4]. A study by Faria-Ribeiro and collaborators observed that both relative sagittal and tangential components of peripheral astigmatism

across the horizontal meridian of the retina of progressing myopes were significantly more hyperopic than in non-progressing myopes [44]. Additionally, they noted that the nasal retinal contour of progressing myopes was steeper than non-progressing myopes. They suggested that the nasal retina might play a more important role in the ocular growth mechanism and possibly be more sensitive to peripheral astigmatic defocus [44]. Regarding those findings from Howland [7] and Faria-Ribeiro et al. [44], it is possible that the meridional effect observed in the present study may be related not only to the radial distribution of the cells, but also to the presence of uncorrected off-axis astigmatism (symbiosis between optical and neural components of the eye), which may have implications for future studies on myopia progression and management.

The measurement and correction of off-axis astigmatism and the evaluation of the retinal activity by meridians and hemifields (nasal versus temporal retina) in both conditions (uncorrected and corrected off-axis astigmatism) may add new future perspectives on the influence of the peripheral retina on the visual system. Therefore, this could also bring other approaches to the progression, development and control of myopia based on the hypothesis that correcting the peripheral refractive errors would enhance the contrast and increase the ability to detect and resolve spatial image cues. Some inner retinal cells presenting radial orientation show preferential orientation and maximize the contrast of grids in the periphery [5], which allows for enlarging the alignment zone.

The current study showed no differences in PERG responses with different grid orientations. One could assume that the ganglion cells responded according to the information from the photoreceptors and bipolar cells. However, in both PERG and total mfERG responses, the weight of the macular information overlaps that of the other retinal areas due to its higher cell density. This means that possible changes beyond the macula end up being masked by the macular area. Nevertheless, since the processing of the orientation features is more related to the inner retinal layers [40,42], it is possible that the evaluation of the local and meridional response of ganglion cells would mirror similar results to those found with the mfERG technique. Such results might be present when using the multifocal PERG technique [48], which was not used in the present study.

Throughout the data analysis, we acknowledge some gaps and limitations in this study. Although the sample size was enough to guarantee the statistical power of 80%, increasing the number of participants could decrease the disparity of values among subjects. However, one must consider that the distribution of electrophysiological data is non-normal, since there could be large inter-subject differences and even small within-subject variations. Despite the variability observed in some of the variables as high IQR values compared to the median values (Table 3), the behavior we measured was consistent, and all subjects showed changes in the same direction, though of different magnitude. Therefore, despite the variability presented and the need to increase sample size in future studies, we are confident that we are reporting consistent responses to the changes in stimuli orientation.

In both experiments, mfERG and PERG were used to access the response of the outer and inner retinal layers, respectively. A better option could be to use global flash mfERG, like Chin et al. [21], which allows for simultaneous access to the outer (direct component, DC) and inner (induced component, IC) retinal response in multiple areas. This technique would minimize differences related to using different stimulation parameters, decrease the time of the research protocol and, consequently, reduce the subject's discomfort. Additionally, it is possible that the global flash mfERG technique would allow for observing the meridional sensitivity of the retina to gratings orientation in both outer and inner layers, which in this study was only observed in the outer layers with the standard mfERG.

Transparent films printed with square grids were placed over the stimuli presented in the monitor's display for the two experiments of this study. Several psychophysical studies prefer sinusoidal grids because these are probably the visual equivalent of a so-called pure tone [49] (the light intensity of the bars pattern varies in a sinusoidal manner). Some studies showed that using sinusoidal grids in a circular window gives better spatial frequency detection values [50,51]. However, it is possible that the visual system does not perceive

differences between square and sinusoidal disparity grids below the threshold [52] and may prefer square rather than sine waves because of the mechanisms of lateral inhibition in the retina and visual cortex [53]. This may suggest that the type of grids may not be so relevant for the two experiments here.

5. Conclusions

This study presents a new paradigm of meridional analysis of mfERG results that might be more sensitive to orientation changes than the traditional strategies involving quadrants or hemifield aggregation and averaging hexagonal receptive field areas.

The results of the current study suggest that there is a local meridional effect mechanism for detecting stimulus orientation, since there was higher responsivity of the retinal meridians to grids parallel to the meridian, whilst grids of opposite orientation decreased it the most.

These results may have future implications for myopia research since the radial distribution of the cells and off-axis uncorrected astigmatism may play an important role in visual processing mechanisms in the different retinal layers. This strategy was sensitive to detect changes in the outer retina electrophysiological activity with variations in stimulus orientation.

Author Contributions: Conceptualization, A.A.-d.-S., P.F. and J.M.G.-M.; Methodology, A.A.-d.-S., P.F., A.Q., N.L.-G. and J.M.G.-M.; Software, A.A.-d.-S. and A.Q.; Validation, A.A.-d.-S.; Formal Analysis, A.A.-d.-S., A.Q. and N.L.-G.; Investigation, A.A.-d.-S.; Resources, J.M.G.-M.; Data Curation, A.A.-d.-S. and A.Q.; Writing—Original Draft Preparation, A.A.-d.-S.; Writing—Review and Editing, A.Q., P.F., N.L.-G. and J.M.G.-M.; Visualization, A.A.-d.-S.; Supervision, A.Q., N.L.-G. and J.M.G.-M.; Project Administration, P.F. and J.M.G.-M.; Funding Acquisition, A.A.-d.-S., A.Q., P.F. and J.M.G.-M. All authors have read and agreed to the published version of the manuscript.

Institutional Review Board Statement: The study was conducted according to the guidelines of the Declaration of Helsinki and approved by the Ethics Committee) for Health and Life Sciences of the University of Minho.

Informed Consent Statement: Informed consent was obtained from all subjects involved in the study.

Data Availability Statement: The data presented in this study are available on request from the corresponding author.

Conflicts of Interest: The authors declare no conflict of interest.

References

1. Gwiazda, J.; Grice, K.; Held, R.; McLellan, J.; Thorn, F. Astigmatism and the development of myopia in children. *Vis. Res.* **2000**, *40*, 1019–1026. [CrossRef]
2. Serrano-Pedraza, I.; Grady, J.P.; Read, J.C.A. Spatial frequency bandwidth of surround suppression tuning curves. *J. Vis.* **2012**, *12*, 24. [CrossRef]
3. Queirós, A.; Amorim-De-Sousa, A.; Lopes-Ferreira, D.; Villa-Collar, C.; Gutiérrez, R.; González-Méijome, J.M. Relative peripheral refraction across 4 meridians after orthokeratology and LASIK surgery. *Eye Vis.* **2018**, *5*, 12. [CrossRef] [PubMed]
4. Atchison, D.A.; Pritchard, N.; Schmid, K.L. Peripheral refraction along the horizontal and vertical visual fields in myopia. *Vis. Res.* **2006**, *46*, 1450–1458. [CrossRef]
5. Charman, W.N. Myopia, posture and the visual environment. *Ophthalmic Physiol. Opt.* **2011**, *31*, 494–501. [CrossRef]
6. Kee, C.-S.; Hung, L.-F.; Qiao-Grider, Y.; Roorda, A.; Smith, E.L. Effects of Optically Imposed Astigmatism on Emmetropization in Infant Monkeys. *Investig. Ophthalmol. Vis. Sci.* **2004**, *45*, 1647–1659. [CrossRef]
7. Howland, H.C. A possible role for peripheral astigmatism in the emmetropization of the eye. In Proceedings of the 13th International Myopia Conference, Tubingen, Germany, 26–29 July 2010.
8. Hung, L.-F.; Ramamirtham, R.; Huang, J.; Qiao-Grider, Y.; Smith, E.L. Peripheral Refraction in Normal Infant Rhesus Monkeys. *Investig. Ophthalmol. Vis. Sci.* **2008**, *49*, 3747–3757. [CrossRef]

9. Smith, E.I.; Greeman, N.; Ho, A.; Holden, B. Methods and Apparatuses for Altering Relative Curvature of Field and Positions of Peripheral, off-Axis Focal Positions. U.S. Patent 7.025.460 B2, 25 June 2006.
10. Pärssinen, O. Astigmatism and school myopia. *Acta Ophthalmol.* **2009**, *69*, 786–790. [CrossRef] [PubMed]
11. Chamberlain, P.; Peixoto-De-Matos, S.C.; Logan, N.S.; Ngo, C.; Jones, D.; Young, G. A 3-year Randomized Clinical Trial of MiSight Lenses for Myopia Control. *Optom. Vis. Sci.* **2019**, *96*, 556–567. [CrossRef] [PubMed]
12. Queirós, A.; Lopes-Ferreira, D.; González-Méijome, J.M. Astigmatic Peripheral Defocus with Different Contact Lenses: Review and Meta-Analysis. *Curr. Eye Res.* **2016**, *41*, 1005–1015. [CrossRef]
13. González-Méijome, J.M.; Peixoto-De-Matos, S.C.; Faria-Ribeiro, M.; Lopes-Ferreira, D.P.; Jorge, J.; Legerton, J.; Queiros, A. Strategies to Regulate Myopia Progression with Contact Lenses: A review. *Eye Contact Lens Sci. Clin. Pract.* **2016**, *42*, 24–34. [CrossRef]
14. Queirós, A.; González-Méijome, J.M.; Jorge, J.; Villa-Collar, C.; Gutiérrez, A.R. Peripheral Refraction in Myopic Patients after Orthokeratology. *Optom. Vis. Sci.* **2010**, *87*, 323–329. [CrossRef]
15. Gifford, K.L.; Gifford, P.; Hendicott, P.L.; Schmid, K. Stability of peripheral refraction changes in orthokeratology for myopia. *Contact Lens Anterior Eye* **2019**, *43*, 44–53. [CrossRef] [PubMed]
16. Pauné, J.; Queiros, A.; Lopes-Ferreira, D.; Faria-Ribeiro, M.; Quevedo, L.; Gonzalez-Meijome, J.M. Efficacy of a Gas Permeable Contact Lens to Induce Peripheral Myopic Defocus. *Optom. Vis. Sci.* **2015**, *92*, 596–603. [CrossRef]
17. Amorim-De-Sousa, A.; Schilling, T.; Fernandes, P.; Seshadri, Y.; Bahmani, H.; González-Méijome, J.M. Blue light blind-spot stimulation upregulates b-wave and pattern ERG activity in myopes. *Sci. Rep.* **2021**, *11*, 9273. [CrossRef] [PubMed]
18. Queirós, A.; Pereira-Da-Mota, A.F.; Costa, J.; Amorim-De-Sousa, A.; Fernandes, P.R.B.; González-Méijome, J.M. Retinal Response of Low Myopes during Orthokeratology Treatment. *J. Clin. Med.* **2020**, *9*, 2649. [CrossRef] [PubMed]
19. Amorim-De-Sousa, A.; Macedo-De-Araújo, R.; Fernandes, P.; Queirós, A.; González-Méijome, J.M. Multifocal Electroretinogram in Keratoconus Patients without and with Scleral Lenses. *Curr. Eye Res.* **2021**, *46*, 1732–1741. [CrossRef] [PubMed]
20. Kader, M.A. Electrophysiological study of myopia. *Saudi J. Ophthalmol.* **2011**, *26*, 91–99. [CrossRef]
21. Chin, M.P.; Chu, P.H.W.; Cheong, A.M.Y.; Chan, H.H.L. Human Electroretinal Responses to Grating Patterns and Defocus Changes by Global Flash Multifocal Electroretinogram. *PLoS ONE* **2015**, *10*, e0123480. [CrossRef]
22. Ho, W.-C.; Wong, O.-Y.; Chan, Y.-C.; Wong, S.-W.; Kee, C.-S.; Chan, H.H.-L. Sign-dependent changes in retinal electrical activity with positive and negative defocus in the human eye. *Vis. Res.* **2012**, *52*, 47–53. [CrossRef]
23. Trick, G.L.; Wintermeyer, D.H. Spatial and temporal frequency tuning of pattern-reversal retinal potentials. *Investig. Ophthalmol. Vis. Sci.* **1982**, *23*, 774–779.
24. Odom, J.V.; Maida, T.M.; Dawson, W.W. Pattern evoked retinal response (PERR) in human: Effects of spatial frequency, temporal frequency, luminance and defocus. *Curr. Eye Res.* **1982**, *2*, 99–108. [CrossRef] [PubMed]
25. Sachs, M.B.; Nachmias, J.; Robson, J.G. Spatial-Frequency Channels in Human Vision. *J. Opt. Soc. Am.* **1971**, *61*, 1176–1186. [CrossRef] [PubMed]
26. Greenlee, M.W. Spatial frequency discrimination of band-limited periodic targets: Effects of stimulus contrast, bandwidth and retinal eccentricity. *Vis. Res.* **1992**, *32*, 275–283. [CrossRef] [PubMed]
27. Hood, N.C.; Frishman, L.J.; Saszik, S.; Viswanathan, S. Retinal origins of the primate multifocal ERG: Implications for the human response. *Investig. Ophthalmol. Vis. Sci.* **2002**, *43*, 1673–1685.
28. Hood, D.C. Assessing retinal function with the multifocal technique. *Prog. Retin. Eye Res.* **2000**, *19*, 607–646. [CrossRef]
29. Thompson, D.; Drasdo, N. The origins of luminance and pattern responses of the pattern electroretinogram. *Int. J. Psychophysiol.* **1994**, *16*, 219–227. [CrossRef]
30. Burkhardt, D.A. Contrast processing by ON and OFF bipolar cells. *Vis. Neurosci.* **2010**, *28*, 69–75. [CrossRef]
31. Bach, M.; Brigell, M.G.; Hawlina, M.; Holder, G.E.; Johnson, M.A.; McCulloch, D.; Meigen, T.; Viswanathan, S. ISCEV standard for clinical pattern electroretinography (PERG): 2012 update. *Doc. Ophthalmol.* **2012**, *126*, 1–7. [CrossRef]
32. Hoffmann, M.B.; Bach, M.; Kondo, M.; Li, S.; Walker, S.; Holopigian, K.; Viswanathan, S.; Robson, A.G. ISCEV standard for clinical multifocal electroretinography (mfERG) (2021 update). *Doc. Ophthalmol.* **2021**, *142*, 5–16. [CrossRef]
33. Hood, D.C.; Bach, M.; Brigell, M.; Keating, D.; Kondo, M.; Lyons, J.S.; Marmor, M.F.; McCulloch, D.L.; Plamowski-Wolfe, A.M. ISCEV standard for clinical multifocal electroretinography (mfERG) (2011 edition). *Doc. Ophthalmol.* **2012**, *124*, 1–13. [CrossRef]
34. Amorim-De-Sousa, A.; Moreira, L.; Macedo-De-Araújo, R.; Amorim, A.; Jorge, J.; Fernandes, P.R.; Queirós, A.; González-Méijome, J.M. Impact of contact lens materials on the mfERG response of the human retina. *Doc. Ophthalmol.* **2019**, *140*, 103–113. [CrossRef]
35. Mazinani, B.A.E.; Repas, T.; Weinberger, A.W.A.; Vobig, M.A.; Walter, P. Amplitude calculation in multifocal ERG: Comparison of repeatability in 30 Hz flicker and first order kernel stimulation. *Graefe's Arch. Clin. Exp. Ophthalmol.* **2006**, *245*, 338–344. [CrossRef]
36. Yoshii, M.; Yanashima, K.; Wakaguri, T.; Sakemi, F.; Kikuchi, Y.; Suzuki, S.; Okisaka, S. A basic investigation of multifocal electroretinogram: Reproducibility and effect of luminance. *Jpn. J. Ophthalmol.* **2000**, *44*, 122–127. [CrossRef] [PubMed]
37. Schimitzek, T.; Bach, M. The influence of luminance on the multifocal ERG. *Doc. Ophthalmol.* **2006**, *113*, 187–192. [CrossRef] [PubMed]
38. Korth, M. Pattern-evoked responses and luminance-evoked responses in the human electroretinogram. *J. Physiol.* **1983**, *337*, 451–469. [CrossRef] [PubMed]
39. Schall, J.; Perry, V.; Leventhal, A. Retinal ganglion cell dendritic fields in old-world monkeys are oriented radially. *Brain Res.* **1986**, *368*, 18–23. [CrossRef]

40. Sasaki, Y.; Rajimehr, R.; Kim, B.W.; Ekstrom, L.B.; Vanduffel, W.; Tootell, R.B. The Radial Bias: A Different Slant on Visual Orientation Sensitivity in Human and Nonhuman Primates. *Neuron* **2006**, *51*, 661–670. [CrossRef]
41. Sjöstrand, J.; Popovic, Z.; Conradi, N.; Marshall, J. Morphometric study of the displacement of retinal ganglion cells subserving cones within the human fovea. *Graefe's Arch. Clin. Exp. Ophthalmol.* **1999**, *237*, 1014–1023. [CrossRef]
42. Venkataraman, A.P.; Winter, S.; Rosén, R.; Lundström, L. Choice of Grating Orientation for Evaluation of Peripheral Vision. *Optom. Vis. Sci.* **2016**, *93*, 567–574. [CrossRef]
43. Jonas, J.B.; Ang, M.; Cho, P.; Guggenheim, J.A.; He, M.G.; Jong, M.; Logan, N.S.; Liu, M.; Morgan, I.; Ohno-Matsui, K.; et al. IMI Prevention of Myopia and Its Progression. *Investig. Ophthalmol. Vis. Sci.* **2021**, *62*, 6. [CrossRef]
44. Faria-Ribeiro, M.; Queiros, A.; Lopes-Ferreira, D.; Jorge, J.; Gonzalez-Meijome, J.M. Peripheral Refraction and Retinal Contour in Stable and Progressive Myopia. *Optom. Vis. Sci.* **2013**, *90*, 9–15. [CrossRef] [PubMed]
45. Wallman, J.; Winawer, J. Homeostasis of Eye Growth and the Question of Myopia. *Neuron* **2004**, *43*, 447–468. [CrossRef]
46. Neil Charman, W.; Radhakrishnan, H. Peripheral refraction and the development of refractive error: A review. *Ophthalmic Physiol. Opt.* **2010**, *30*, 321–338. [CrossRef] [PubMed]
47. Vyas, S.A.; Kee, C.-S. Early Astigmatism Can Alter Myopia Development in Chickens. *Investig. Ophthalmol. Vis. Sci.* **2021**, *62*, 27. [CrossRef] [PubMed]
48. Langrová, H.; Jägle, H.; Zrenner, E.; Kurtenbach, A. The multifocal pattern electroretinogram (mfPERG) and cone-isolating stimuli. *Vis. Neurosci.* **2007**, *24*, 805–816. [CrossRef] [PubMed]
49. von Helmholtz, H.L.F. *On the Sensations of Tone as a Physiological Basis for the Theory of Music*; Longmans, Green, and Co.: London, UK, 1875.
50. Thibos, L.N.; Still, D.L.; Bradley, A. Characterization of spatial aliasing and contrast sensitivity in peripheral vision. *Vis. Res.* **1996**, *36*, 249–258. [CrossRef] [PubMed]
51. Campbell, F.W.; Carpenter, R.H.S.; Levinson, J.Z. Visibility of aperiodic patterns compared with that of sinusoidal gratings. *J. Physiol.* **1969**, *204*, 283–298. [CrossRef]
52. Allenmark, F.; Read, J.C.A. Detectability of sine- versus square-wave disparity gratings: A challenge for current models of depth perception. *J. Vis.* **2010**, *10*, 17. [CrossRef] [PubMed]
53. Campbell, F.W.; Robson, J.G. Application of fourier analysis to the visibility of gratings. *J. Physiol.* **1968**, *197*, 551–566. [CrossRef]